Future Computing and Informatics Journal

Volume 3
Issue 2 *Vol 3,Issue 2,2018*

Article 16

2018

Fuzzy clustering based transition region extraction for image segmentation

Priyadarsan Parida
GIET University, priyadarsan.vssut@gmail.com

Available online at www.sciencedirect.com

ScienceDirect

Future Computing and Informatics Journal 3 (2018) 321−333
http://www.journals.elsevier.com/future-computing-and-informatics-journal/

Fuzzy clustering based transition region extraction for image segmentation

Priyadarsan Parida

Department of Electronics & Communication Engineering, Gandhi Institute of Engineering and Technology, Gunupur, Rayagada, Odisha, 765022, India

Received 8 January 2018; accepted 18 October 2018
Available online 7 November 2018

Abstract

Transition region based approaches are recent hybrid segmentation techniques well known for its simplicity and effectiveness. Here, the segmentation effectiveness depends on robust extraction of transition regions. So, we have proposed clustering approach based transition region extraction method for image segmentation. The proposed method initially uses the local variance of the input image to get the variance feature image. Fuzzy C-means clustering is applied to the variance feature image to separate the transitional features from the feature image. Further, Otsu thresholding is applied to the transitional feature image to extract the transition region. For extracting the exact edge image, morphological thinning operation is performed. The edge image extracted in former step is closed in nature. The morphological cleaning and region filling operation is performed on an edge image to get the object regions. Finally, objects are extracted via these object regions. The proposed method is compared with different image segmentation methods. An experimental result reveals that the proposed method outperforms other methods for segmentation of images containing single and multiple objects.

Keywords: Transition region; Otsu thresholding; Clustering

1. Introduction

Image segmentation is an important pre-processing step for all computer vision and image understanding tasks. It has wide a range of applications such as biometrics [1], medical image analysis [2], crop disease detection and classification [3] etc. Image segmentation is the process of separating the object (foreground) from background considering certain features of the image such as colour, intensity, texture etc. In the past decade, a wide variety of segmentation techniques are available in the literature. In recent era a number of hybrid segmentation techniques have been emerged which provide better segmentation results in comparison to that of the traditional methods. These hybrid segmentations are classified as model based segmentation approaches [4,5], machine learning approaches [6], graph-cut methods [7], active contour and level set methods [8−10] and transition region based approaches [11−17]. In model based approaches, the image is characterized by a statistical model and the model parameters are used as features for segmentation [8]. The machine learning process is basically a training process where a network is trained to optimize the weights of the network from training images features like texture, brightness, etc. After training, the network is presented the query image and it performs classification based segmentation from the tuned weights and learned weights [6]. Graph cut based approaches consider the image as a weighted graph with nodes and vertices, where nodes represent pixels or voxels and vertices represent the neighbourhood relationship between pixels. A cost function which represents the cut is optimal in the sense that it effectively separates the object from the background [7]. Active contour based approaches deform its shape in the presence of external and internal forces leading the contour towards object [9]. In edge-based active contour methods

E-mail address: priyadarsan.vssut@gmail.com.
Peer review under responsibility of Faculty of Computers and Information Technology, Future University in Egypt.

https://doi.org/10.1016/j.fcij.2018.10.002

image gradient is used to detect object boundaries [18] whereas region-based active contours use the object and background regions to find an energy optimum where the model fits the image to its best [11]. Level set methods usually make use of an edge indicator to pull the zero level set in the direction of the desired object boundaries [9]. Transition region based methods [13−16,19,20] uses transition region for segmentation of images. In local entropy (LE) based method [19] the entropy of a neighbourhood is considered to determine the transition region. It has a limitation that in the event of frequent changes in gray level in a local area, it increases the local entropy and the pixels in the neighbourhood is identified as the transition region and it belongs to the foreground or the background. To overcome these disadvantages, Li et al. [13] developed a method for local extraction of the transition region based on the gray level difference (LGLD) which takes into account both changes in gray levels and the extent of these changes. However, the parameter selection unit for determining the threshold value is a problem. The modified local entropy method (MLE) [14] was then put in place to improve the extraction of the transition region. This method also suffers from the same problem as in LGLD. These techniques are ineffective when the foreground and background are of varying intensities. Furthermore, these are mainly used for images that contain a single object. A recent transition region based method named robust single-object image segmentation (RIB) proposed by Zuoyong Li et al. [15] is based on salient transition region provides good segmentation results. But, it only applies to images that contain a single object. In order to mitigate the limitation, Parida et al. [16] proposed local variance and morphological operator based method to yield better performance for both single and multiple object segmentation. In this method, the images are categorized into four classes based on whether the background and foreground are simple or textured. The performance of the method degrades when the method is applied on images with (i) textured background and (ii) overlapping gray levels between foreground and background. In order to improve the performance, Parida et al. [20] proposed a novel method using 2-D Gabor filters for transition region. This method works well for overlapping gray levels between background and foreground. The method is unable to perform well when the image contains textured background. Also, it has been found that the proposed method [20] cannot outperform Parida et al. [16] when both the background and foreground are simple.

Clustering is one of the basic approach used for segmentation purpose. A number of clustering based segmentation algorithm is available in the literature [21,22]. The clustering approaches developed so far are divided into two types: (a) crisp set clustering where each point of data is restricted to be clustered to exclusively in one cluster. (b) Fuzzy clustering approach where data points are clustered according to fuzzy set involving partial membership concept. Fuzzy c-means clustering approach is one of the most widely used clustering approaches used for partitioning the data sets into a distinct number of disjoint sets where each set of data points are independent of each other [22]. The transition region approaches for segmentation emphasize on accurate extraction of the transition region. Better transition region provides better image segmentation. So, here we have proposed a method for extraction of transition region using fuzzy c-means clustering which gives better segmentation. The extraction of transition region by the proposed method is demonstrated in Figs. 1−4. Here, the result is compared with recently developed transition region based methods e.g. RIB, Parida et al. [16] and Parida et al. [20]. All the methods are tested on Boat and Puppy images taken from MSRM dataset [23]. The transition region by different methods on Boat image is shown in Fig. 1. A region 'R' indicated by circle is detected where the transition region of proposed method is continuous as compared to others. This can be better examined by looking the zoomed version of the indicated regions which are shown from Fig. 1(f)−(i). The double headed arrow marked with red colour shows the point of continuity (continuous or discontinuous). As the proposed method gives better transition region, the segmentation result is also better as compared to other methods which can be revealed from Fig. 2.

The methods are also tested on Puppy image and results are shown in Figs. 3 and 4. It has been found that transition region of the proposed method suppresses the background textures effectively as compared to other methods. The effectiveness of segmentation result is demonstrated in Fig. 4.

The rest of the paper is organized as follows: Section 2 describes the proposed method briefly. The various performance measures used for evaluating the segmentation result are discussed in Section 3. The Section 4 explains the reason for using 3-class fuzzy c-means clustering. The experimental results and discussion is given in Section 5. Finally the paper concludes in Section 6.

2. Proposed method

The proposed method starts with the local variance feature extraction of the original gray image. The local features extracted divide the input image to different intensity levels. Further a three class fuzzy c-means clustering approach is applied to feature image to extract three different intensity levels. This leads to easier extraction of the transition region between foreground and background. Morphological thinning and region filling operation is employed in the transition region to extract the object regions. Finally, objects are extracted via these object regions. Fig. 5 shows the architecture of the proposed method.

2.1. Local variance feature extraction

Initially from the original image the local variance features are extracted. The region behind extracting local variance features is that the area having higher variance generally

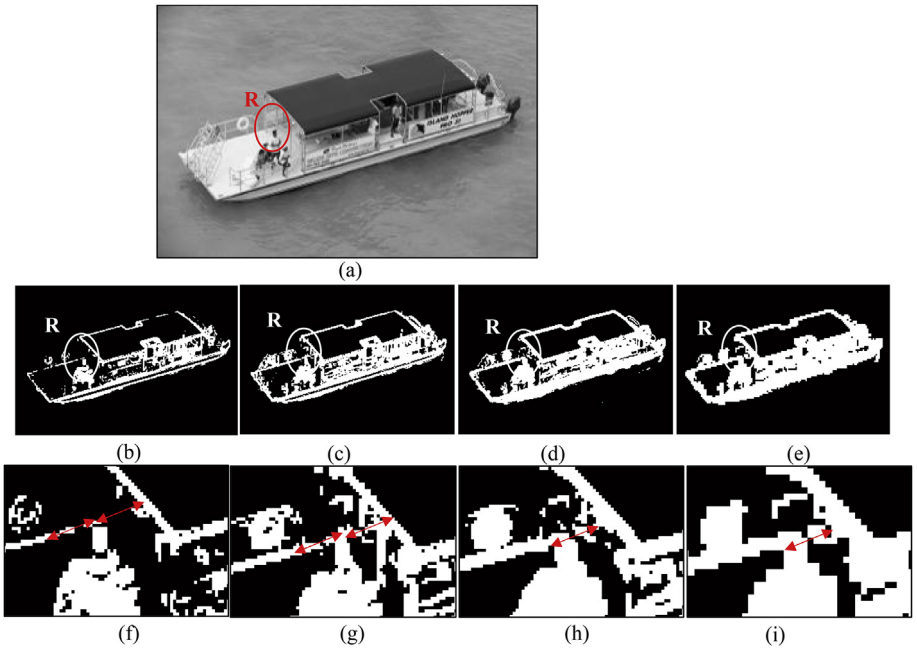

Fig. 1. Transition region extraction of Boat image: (a) Original gray image, (b) RIB, (c) [16], (d) [20], (e) Proposed method, (f) – (i) zoomed region R of (b)–(e).

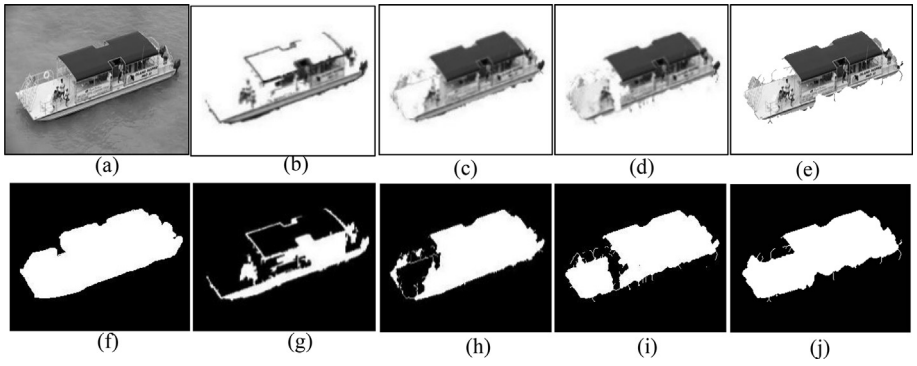

Fig. 2. Segmentation result and segmentation mask of Boat image for various methods: (a) Original image, (b)–(e) Segmentation result of different methods: (b) RIB, (c) [16], (d) [20], (e) Proposed method, (f) Ground truth, (g)–(j) Segmentation mask of different methods: (g) RIB, (h) [16], (i) [20], (j) Proposed method.

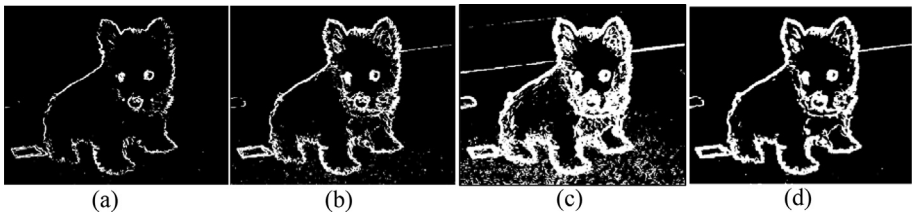

Fig. 3. Transition region of different methods of Puppy image: (a) RIB, (b) [16], (c) [20], (d) Proposed method.

contains the edge of the object regions where as homogeneous regions has less variance in comparison to the edge regions [16]. For a $n \times n$ local neighbourhood, having central pixel $x(k,l)$ the local variance features are extracted as

$$Lv(k,l) = \sigma^2 = \frac{1}{n^2-1}\sum_{x=1}^{n}\sum_{y=1}^{n}\left(f(x,y)-\bar{f}\right)^2 \text{ for } \begin{matrix} k=1,2,....,M \\ l=1,2,....,N \end{matrix} \quad (1)$$

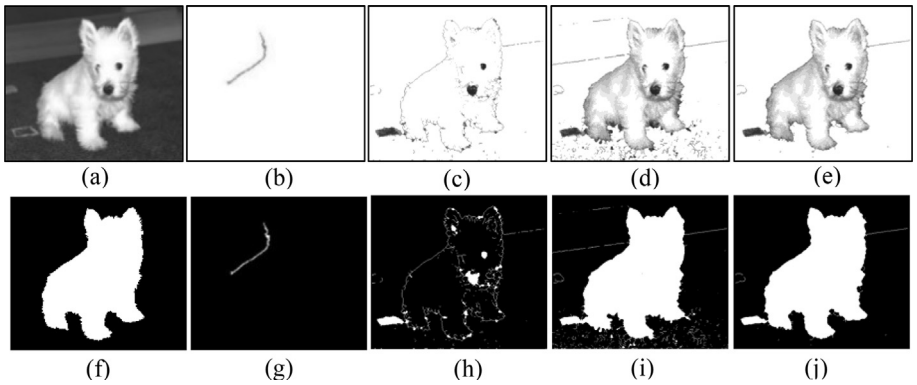

Fig. 4. Segmentation result and segmentation mask of Puppy image for various methods: (a) Original image, (b)–(e) Segmentation result of different methods: (b) RIB, (c) [16], (d) [20], (e) Proposed method, (f) Ground truth, (g)–(j) Segmentation mask of different methods: (g) RIB, (h) [16], (i) [20], (j) Proposed method.

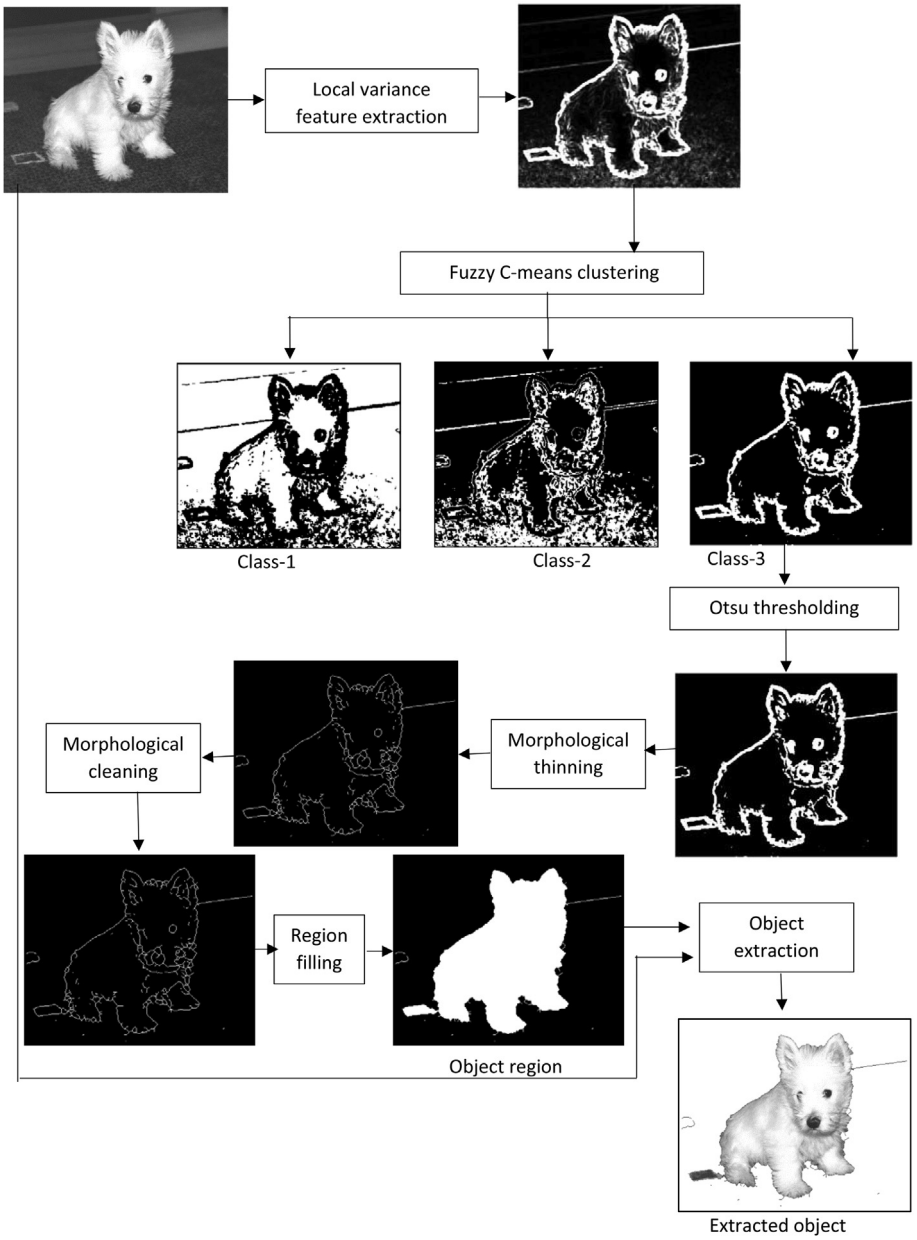

Fig. 5. Architecture of proposed method.

where, (x, y) indicate coordinate of local neighbourhood of $n \times n$ sub image f and the symbol $\overline{f}$ is the gray level mean of the neighbourhood. Equation (1) is applied throughout the image by sliding the window $n \times n$ from left to right and top to bottom to achieve the local variance feature image. The height and width of the image is denoted by M and N respectively. The local variance feature image represents only dominating features such as edge of objects as well as the background features which are further clustered.

2.2. Fuzzy c-mean clustering to extract the transitional features

The local features extracted from the former step undergoes clustering to extract the transitional features. Clustering techniques search the similarities between pixels or a cluster of pixels for finding distinct structures in feature space. It basically partitions a set of pixels from the input feature space in a homogeneous group of pixels [24]. The Fuzzy c-means (FCM) clustering algorithm is one of the widely used unsupervised clustering algorithm due to its simplicity. Here the clustering is applied to the variance features. The features consist of background features, transitional features and interior object texture features. We have used a 3-class FCM algorithm to the feature image. The reason of choosing 3-class clustering is discussed in Section 4. The first class separate out the background features. The second class separates out the inside texture features present in object regions as well as some texture features in background portion. The third class separates the middle portion of the second class features basically called the transitional features. The separation is better shown in Fig. 6.

Fig.6(a) and Fig.6(c) shows the feature image for Eagle and Puppy image. Fig.6(b) and Fig.6(d) shows the class separation of features based on 3-class FCM for Eagle and Puppy image. The red region is first class partition of FCM clustering. From the figure it can be clearly understood that it simply represents the background regions. The green colour regions are second class partition sets indicating the inner prominent texture regions of object regions as well as the outer background texture regions. The blue regions indicate the transitional features which lie on the boundary between the objects and background. Finally, at the end of the clustering process, we achieve three different classes of features out of which we choose class-3 features which is called transition features for subsequent processing. The individual class separation demonstration is given in Fig. 7.

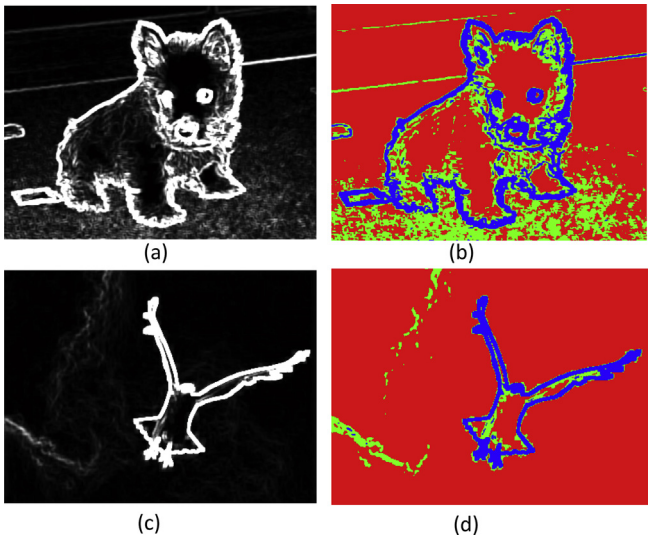

Fig. 6. Feature image and clustering output for Puppy and Eagle image: (a) Feature of Puppy image, (b) 3-class clustering of (a), (c) Feature of Eagle image, (d) 3-class clustering of (c).

The algorithm used for FCM is as follows: the FCM attempts to find a partition (p fuzzy clusters) for a set of features $f_j \in \Re$, $j = 1, 2, .., C$ minimizing the cost function.

$$J(U, M) = \sum_{i=1}^{p} \sum_{j=1}^{C} (U_{i,j})^m d_{i,j} \tag{2}$$

where $U = [U_{i,j}]$ is a fuzzy partition matrix, $U_{i,j} \in [0, 1]$ is the membership coefficient of j^{th} object in i^{th} cluster. The term $M = [m_1, ..., m_p]$ is cluster centre matrix. The term $m \in [1, \infty]$ is referred as fuzzification parameter which is usually set to a value of 2 [25]. The term $d_{i,j} = d(x_j, m_i)$ is the Euclidian distance between x_j and m_i. To summarize our algorithm for feature clustering works in following steps:

(a) Initialize appropriate values for m, c and a small positive integer ε. Select cluster centre M randomly. Initialize step variable $t = 0$.

(b) Evaluate at $t = 0$ or update at $t > 0$ the fuzzy partition matrix U as

$$u_{i,j}^{(t+1)} = \frac{1}{\left(\sum_{l=1}^{p} \left(d_{l,j} / d_{i,j} \right)^{1/(1-m)} \right)} \tag{3}$$

for $i = 1, ..., p$ and $j = 1, ..., C$.

(c) Update the mean matrix M as

$$m_i^{(t=1)} = \left(\sum_{j=1}^{c} \left(u_{i,j}^{t+1} \right)^m x_j \right) \Big/ \left(\sum_{j=1}^{c} \left(u_{i,j}^{t+1} \right)^m \right) \tag{4}$$

for, $i = 1, ..., p$.

(d) Iterate steps (b) − (c) till the following condition is satisfied:

$$\left\| M^{(t+1)} - M^{(t)} \right\| < \varepsilon \tag{5}$$

The number of clusters initialized for our approach is 3. Finally we achieve 3 different clusters of the feature image. The reason for choosing 3-class FCM is discussed in Section 4.

2.3. Extraction of transition regions from transitional features

In the former step we achieve three disjoint sets of features which are categorized as class-1, class-2 and class-3 features.

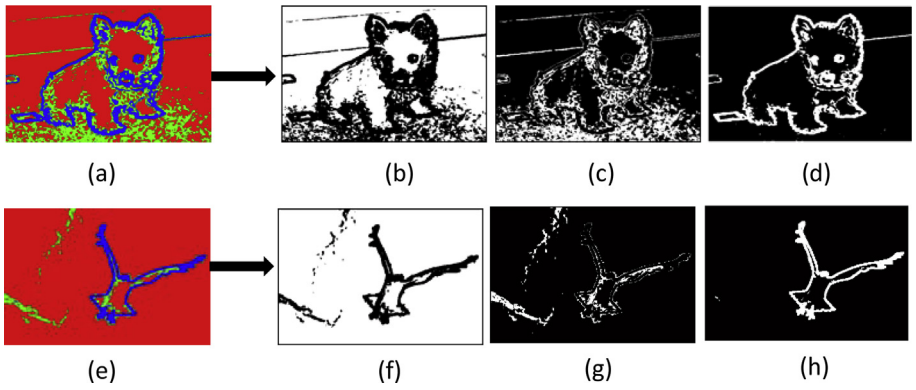

Fig. 7. Separating individual class from 3-class clusters for Puppy and Eagle image: (a) 3-class clustering of Puppy image, (b)–(d) Separation of individual classes from (a), (e) 3-class clustering of Eagle image, (f)–(h) Separation of individual classes from (e).

Class-1 contains only background features. The features of inner object regions and some background regions are classified as class-2 features. The boundary between foreground and background is classified as class-3 features (transitional features). The Otsu thresholding is applied on the class-3 features to get transition region. Finally, at the end of the process a thresholded image is extracted where the value 1 indicates the transition region that separate object from background.

2.4. Morphological thinning and cleaning operation

The transition regions extracted from the former step surround the object regions appropriately. These regions are of several pixels width. So, to achieve a closed object contour of single pixel width, the transition regions are subjected to the morphological thinning operation. The thinning operation results in an edge image of the object along with some isolated pixels near the edge. To get rid of these isolated pixels, morphological cleaning operation is performed. At the end of morphological thinning and cleaning operation, we extract the clean object contours which are continuous in nature.

2.5. Morphological region filling to extract the object regions

The object contours achieved in previous step are fully connected. These further undergoes morphological region filling operation. In this process the inside portion of the edge image is filled with a value of 1 remaining other values as 0. This region filled with values 1 is referred as object regions or segmentation mask.

2.6. Extraction of objects from object regions

The object regions extracted from the former step are a binary image where 1 denote object masks whereas 0 represent background portion. The 1 values are replaced with the original intensity values of gray image to extract the segmented object. The 0 is replaced with intensity value 255 to make the background of the segmented result as white.

3. Performance measures

The performance of the proposed method is quantitatively evaluated via 5 different performance measures: misclassification error (ME) [26,27], false positive rate (FPR) [27], false negative rate (FNR) [27], Jaccard index (JI) [28] and segmentation accuracy (SA) [29].

In a binary classification, the foreground (object) pixels erroneously classified as background or vice versa is termed as misclassification error (ME) [26]. The ME is defined as

$$ME = 1 - \frac{|B_O \cap B_T| + |F_O \cap F_T|}{|B_O| + |F_O|} \tag{6}$$

where, B_O and F_O denote the background and object pixels of ground truth image whereas B_T and F_T represent the background and foreground pixels of the segmentation result. The operator $|.|$ represent cardinality of set operation. The ME value lie between 0 and 1 where 0 represent complete segmentation without any deviation from ground truth. The value 1 correspond to totally erroneous segmentation result. The less the value of ME correspond to better segmentation result. The measures FPR and FNR define the former measure more precisely.

The FPR is the number of background pixels classified as object pixels to the total number of background pixel. The FNR is number of pixels in the object classified in the background pixels to total object pixels. The FPR and FNR is defined as

$$FPR = \frac{|B_O \cap F_T|}{|B_O|} \tag{7}$$

$$FNR = \frac{|F_O \cap B_T|}{|F_O|} \tag{8}$$

The value of FPR and FNR also varies between 0 and 1. The lower the value of FPR and FNR, the better is segmentation result. Higher values of FPR and FNR makes the result to be highly over segmentation and under segmentation respectively.

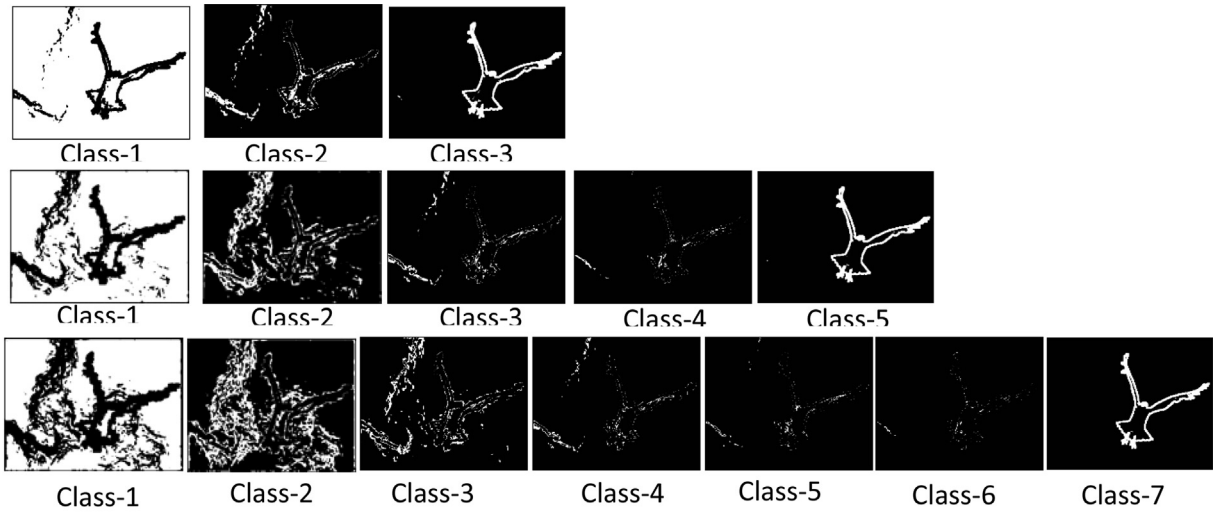

(a) Different class of clustering for Eagle image.

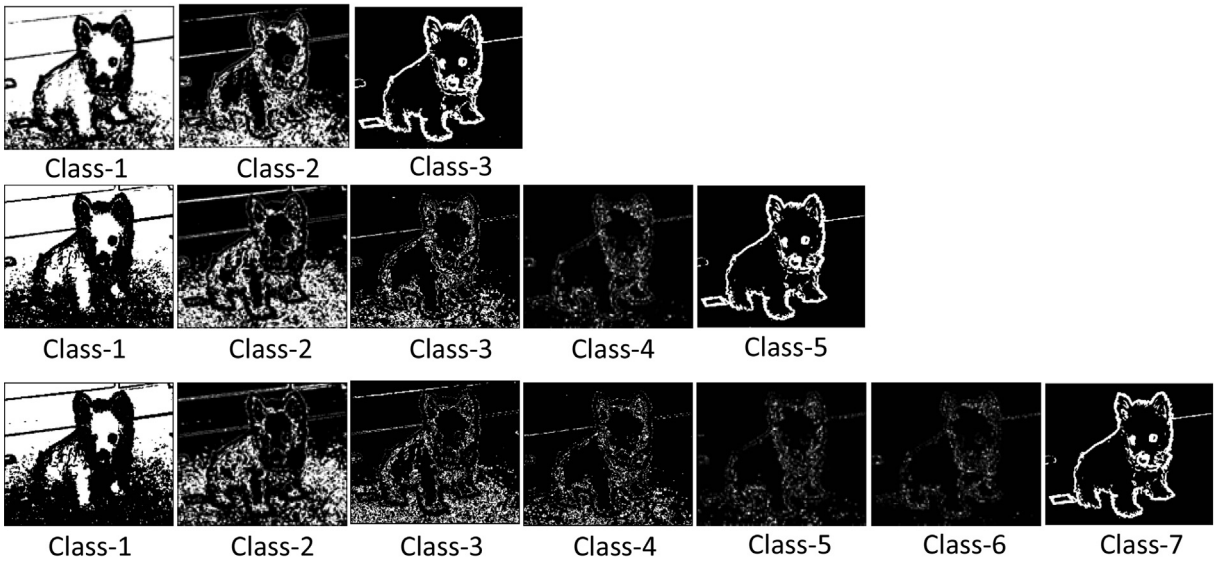

(b) Different class of clustering for Puppy image.

Fig. 8. Effect of higher class clustering for Eagle and Puppy image.

Table 1
Effect of number of classes to performance measures for Eagle and Puppy image.

Image	Number of class	ME	FPR	FNR	JI	SA
Eagle	3-class	0.0083	0.0039	0.0833	0.8583	0.9917
	5-class	0.0080	0.0040	0.0781	0.8627	0.9920
	7-class	0.0079	0.0041	0.0743	0.8648	0.9921
Puppy	3-class	0.0172	0.0199	0.0113	0.9483	0.9828
	5-class	0.3048	0.0169	0.9201	0.0771	0.6952
	7-class	0.3113	0.0171	0.9399	0.0580	0.6887

To evaluate the similarity of the segmentation result with the ground truth Jaccard index is used. The Jaccard index [28] is defined as

$$JI = \frac{|GT \cap SR|}{|GT \cup SR|} \tag{9}$$

where, GT and SR correspond to ground truth and segmentation result respectively. The JI value varies between 0 and 1. Higher value (i.e., close to 1) denote better segmentation result or maximum resemblance with the ground truth (required segmentation result).

Segmentation accuracy (SA) [29] is a global measure which denote the ratio of total well classified pixels in the segmentation result which is given as

$$\text{SA} = \frac{\text{Number of correctly segmented pixels}}{\text{Total number of pixels}} \tag{10}$$

The value of SA remain in the range from 0 to 1. High SA value indicate better segmentation accuracy. Based on the above five performance measures the proposed method is quantitatively compared with various segmentation methods.

Table 2
Performance measures (ME, FPR, FNR, JI, SA) of different methods for various types of images.

Sl. No.	Image	Methods	ME	FPR	FNR	JI	SA
1	Eagle	LE	0.2992	0.3165	0.0000	0.1546	0.7008
		MLE	0.0534	0.0308	0.4460	0.3607	0.9466
		LGLD	0.8009	0.7915	0.9633	0.0025	0.1991
		RIB	0.0159	0.0167	**0.0017**	0.7742	0.9841
		[16]	**0.0065**	0.0047	0.0378	**0.8896**	**0.9935**
		[20]	0.0102	0.0049	0.1013	0.8286	0.9898
		Proposed method	0.0083	**0.0039**	0.0833	0.8583	0.9917
2	Bird	LE	0.0939	0.0990	**0.0072**	0.3696	0.9061
		MLE	0.0654	0.0414	0.4808	0.3028	0.9346
		LGLD	0.9792	0.9901	0.7932	0.0116	0.0208
		RIB	0.0369	0.0202	0.3245	0.5006	0.9631
		[16]	0.0274	0.0192	0.1684	0.6269	0.9726
		[20]	0.0256	0.0148	0.2084	0.6320	0.9744
		Proposed method	**0.0243**	**0.0143**	0.1948	**0.6478**	**0.9757**
3	Boat	LE	0.2435	0.2658	0.1916	0.4993	0.7565
		MLE	0.1871	0.0436	0.5243	0.4316	0.8129
		LGLD	0.7307	0.8330	0.4924	0.1726	0.2693
		RIB	0.1784	0.0121	0.5688	0.4193	0.8216
		[16]	0.0622	0.0017	0.2032	0.7936	0.9378
		[20]	0.0578	0.0021	0.1875	0.8086	0.9422
		Proposed method	**0.0488**	**0.0011**	**0.1600**	**0.8379**	**0.9512**
4	Flower-1	LE	0.5883	0.7238	0.2192	0.2627	0.4117
		MLE	0.3441	0.1458	0.8871	0.0807	0.6559
		LGLD	0.0114	**0.0005**	0.0410	0.9577	0.9886
		RIB	0.0149	0.0202	**0.0006**	0.9471	0.9851
		[16]	0.0184	0.0186	0.0177	0.9349	0.9816
		[20]	0.0167	0.0165	0.0171	0.9406	0.9833
		Proposed method	**0.0100**	0.0081	0.0151	**0.9635**	**0.9900**
5	Papaya	LE	0.5925	0.7658	0.3835	0.3205	0.4075
		MLE	0.3266	0.0638	0.6455	0.3291	0.6734
		LGLD	0.1277	0.0000	0.2816	0.7184	0.8723
		RIB	0.3204	**0.0000**	0.7093	0.2907	0.6796
		[16]	0.0199	0.0153	**0.0254**	0.9570	0.9801
		[20]	0.0195	0.0122	0.0284	0.9576	0.9805
		Proposed method	**0.0177**	0.0007	0.0381	**0.9611**	**0.9823**
6	Players	LE	0.3179	0.3310	0.1492	0.1612	0.6821
		MLE	0.1710	0.1439	0.5243	0.1656	0.8290
		RIB	0.1557	0.0909	1.0000	0.0000	0.8443
		LGLD	0.8065	0.8585	0.1342	0.0716	0.1935
		[16]	0.0824	0.0807	**0.1048**	0.4382	0.9176
		[20]	0.0979	0.0950	0.1357	0.3880	0.9021
		Proposed method	**0.0514**	**0.0432**	0.1580	**0.5405**	**0.9486**
7	Puppy	LE	0.3686	0.4111	0.2777	0.3846	0.6314
		MLE	0.3379	0.0787	0.8941	0.0906	0.6621
		RIB	0.3169	0.0070	0.9821	0.0177	0.6831
		LGLD	0.0191	**0.003**	0.0537	0.9404	0.9809
		[16]	0.3074	0.0201	0.9211	0.0756	0.6926
		[20]	0.0354	0.0443	0.0162	0.8987	0.9646
		Proposed method	**0.0172**	0.0199	**0.0113**	**0.9483**	**0.9828**
8	Flower-2	LE	0.2878	0.2919	0.2599	0.2486	0.7122
		MLE	0.1571	0.0678	0.7633	0.1621	0.8429
		LGLD	0.0161	0.0092	0.0631	0.8818	0.9839
		RIB	0.0141	0.0161	**0.0005**	0.9010	0.9859
		[16]	0.0078	**0.0072**	0.0118	0.9421	0.9921
		[20]	0.0089	0.0084	0.0127	0.9344	0.9911
		Proposed method	**0.0078**	0.0075	0.0100	**0.9421**	**0.9922**
9	Cellphone	LE	0.4343	0.5848	0.1926	0.4164	0.5657
		MLE	0.2929	0.0794	0.6395	0.3193	0.7071
		LGLD	0.1662	**0.0018**	0.4303	0.5681	0.8338
		RIB	0.2540	0.0140	0.6436	0.3485	0.7460
		[16]	0.0248	0.0240	**0.0260**	0.9379	0.9752
		[20]	0.0216	0.0128	0.0357	0.9449	0.9784
		Proposed method	**0.0172**	0.0065	0.0344	**0.9556**	**0.9828**

Table 2 (*continued*)

Sl. No.	Image	Methods	ME	FPR	FNR	JI	SA
10	440	LE	0.4977	0.5180	0.3708	0.1484	0.5023
		MLE	0.1597	0.0993	0.5373	0.2856	0.8403
		LGLD	0.1694	0.1332	0.3956	0.3297	0.8306
		RIB	0.1113	**0.0064**	0.7669	0.2242	0.8887
		[16]	0.0327	0.0205	**0.1089**	**0.7898**	0.9673
		[20]	0.0326	0.0136	0.1517	0.7817	0.9674
		Proposed method	**0.0317**	0.0127	0.1505	0.7871	**0.9683**

4. Reason of choosing 3-class clustering and effects of higher class of clustering

The number of classes for clustering depends on various factors such as computation time and performance measures. For explaining the relationship we have performed a small experiment. If we increase the number of classes in our clustering algorithm, it subsequently increases the computation time due to increase in iteration steps. If we increase the number of classes in clusters, it simply reduces the width of the transition region. This can be verified from the Fig. 8(a) where three different cluster class was applied to the Eagle feature image. The first row of Fig. 8(a) represents the outputs of 3-class clustering approach. The second row shows the results of clustering for 5-class clustering. The third row indicates the clustering result for the same feature image using 7-class clustering approach. From the results it can be concluded that, if we increase in number of classes for clustering the transition region becomes less width only. But in performance point of view the results do not vary much which can be verified from Table 1. In Table 1 the performance measures of Eagle image are calculated for different class clustering. If we increase from 3-class clustering to 7-class clustering, the segmentation accuracy (SA) improves by 0.04%. This indicates that for a low improvement in performance, so it is not wise to increase the number of classes which inherently increases computation time. In case of Puppy image, the performance measures degrades significantly if we increase from 3-class clustering to 7-class clustering. The fact can be verified from Table 1 for Puppy image. Fig. 8(b) shows the clustering results of Puppy image for different class clustering. The above discussion conclude us to choose 3-class clustering rather than higher class clustering.

5. Result and discussion

The entire experiment is performed on a PC with Core-i3, 1.9 GHz processor and 8 GB RAM. The experimentation is done in MATLAB 7.0 environment. The proposed method is compared with several existing transition region based methods such as LE [19], MLE [14], LGLD [13], RIB [15], Parida et al. [16] and Parida et al. [20]. The images used for experimentation are 8-bit and of different resolution to demonstrate the effectiveness of the proposed method. The images are taken from MSRM dataset [23] and Wisemann dataset [30] which contain both single and multiple objects in the experimentation process. The image group used for experimentation has all combinations of foreground (simple or textured) and background (simple or textured). For quantitative evaluation of every image 5 different performance measures (ME, FPR, FNR, JI and SA) are evaluated for all methods along with the proposed method and given in Table 2. For qualitative evaluation the segmented results as well as their segmentation masks along with the original image and ground truth are shown in Fig. 9 and Fig. 10 respectively.

To begin our analysis, for Eagle image where the background sky is having some texture but the foreground is simple. The method [16] attains the best performance except for the FPR and FNR. For Eagle image, the best FNR is given by RIB. The proposed method attains a best FPR value where as other measures are nearly equal, indicating the result of the proposed method is less over-segmented in comparison to the others. The Bird image is having simple foreground and background with two objects. The proposed method has best values of all performance measures except that of FNR. The method LE attains a best FNR value for Bird image, but the visual representation, from Fig. 9 show that the LE method retains most of the foreground region as compared to other methods.

The Boat image has more textured foreground as compared to the background. The proposed method attains best performance measures, indicating that it works better in conditions where the foreground texture dominate the background. The Flower-1 image has simple foreground with background textures. The proposed method attains better performance measure except for FPR and FNR. The lowest FPR is given by method LGLD where as the best FNR is given by RIB. Qualitative results indicate that the proposed method achieve better segmentation result from others, which can be visualized from the segmentation masks in Fig. 10. The Papaya image has textured foreground with simple foreground. The proposed method attains lowest values of ME, JI and SA. The method RIB attains lowest FPR whereas the method [16] attains lowest FNR. Fig. 10 indicate that the major foreground region is missed for RIB method providing under-segmented result. Players image is a multiple object image consisting of complex background, having a field with the crowd. The proposed method achieves best of all performance measures except for the FNR measure. The method [16] attains a best FNR value indicating that the result is slightly under-segmented. But visual inspection of segmentation result as well as segmentation mask from Figs. 9 and 10 reveal that the proposed method results contain less background (present in the upper side of the image) in comparison to other methods. Similarly for Puppy image which has

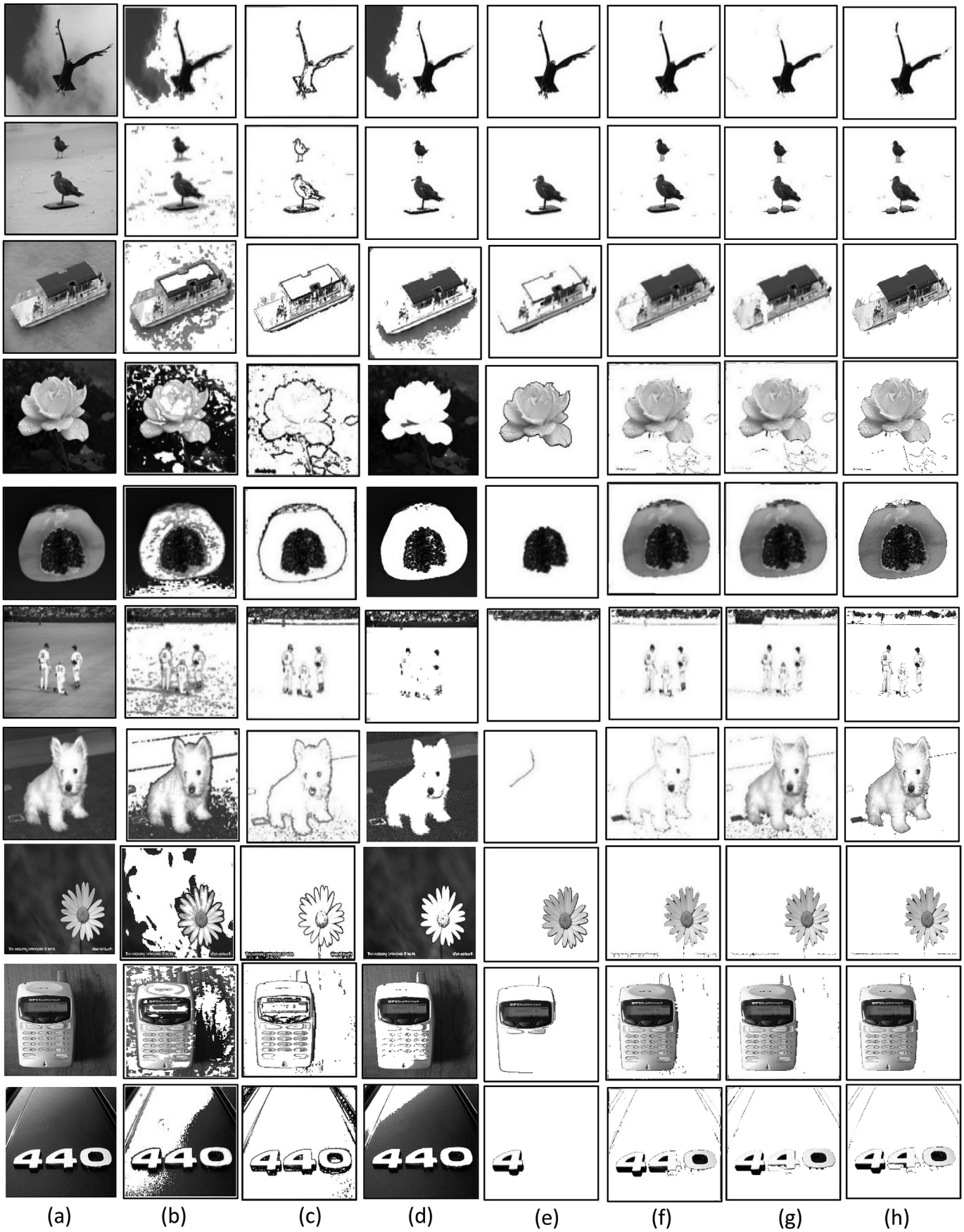

Fig. 9. Segmentation result of various methods for different images: Eagle, Bird, Boat, Flower-1, Papaya, Players, Puppy, Flower-2, Cellphone, 440. (a) Original gray image, (b) LE, (c) MLE, (d) LGLD, (e) RIB, (f) [16], (g) [20], (h) Proposed method.

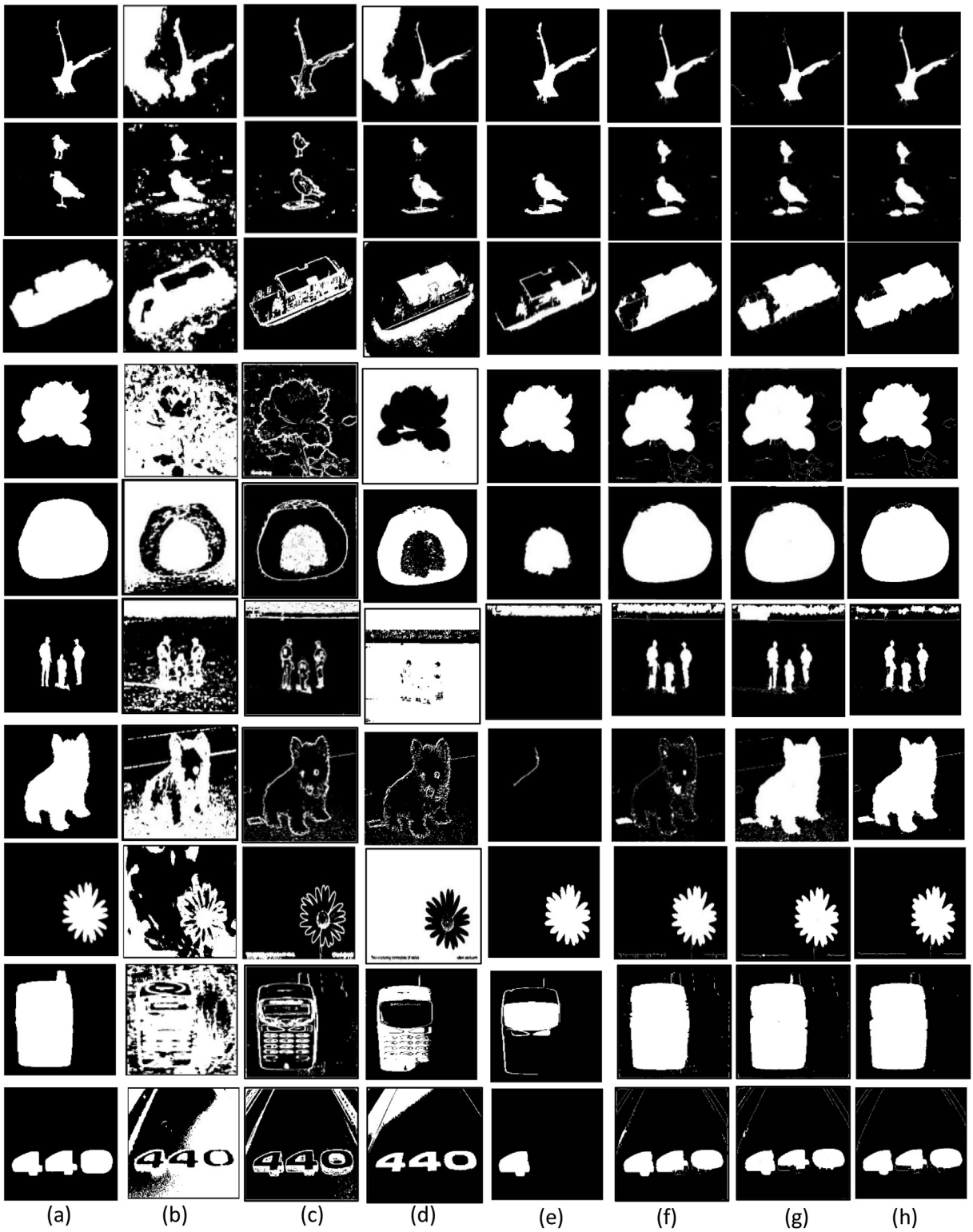

Fig. 10. Segmentation masks of various methods for different images: Eagle, Bird, Boat, Flower-1, Papaya, Players, Puppy, Flower-2, Cellphone, 440. (a) Ground truth, (b) LE, (c) MLE, (d) LGLD, (e) RIB, (f) [16], (g) [20], (h) Proposed method.

both foreground and background textured, the proposed method achieves best measures for all parameters except for the FPR. The method LGLD gives the lowest FPR indicating that the result of the proposed method is slightly over-segmented. But visual inspection from Fig. 10 reveal that LGLD method loses most foreground portion. Similarly for Flower-2 image the proposed method attains best ME, JI and SA. The method [16] achieve lowest FPR indicating that the result of the proposed method is over-segmented than [16]. The method RIB gives the lowest FNR indicating that the result of the proposed method is

Table 3
Average performance of different methods for various performance measures.

Method	Average ME	Average FPR	Average FNR	Average JI	Average SA
LE	0.3724	0.4308	0.2052	0.2966	0.6276
MLE	0.2095	0.0795	0.6342	0.2528	0.7905
LGLD	0.3474	0.2857	0.5443	0.3660	0.6526
RIB	0.1772	0.0967	0.3204	0.5418	0.8229
[16]	0.0590	0.0212	0.1625	0.7386	0.9411
[20]	0.0326	0.0225	0.0895	0.8115	0.9674
Proposed method	**0.0234**	**0.0118**	**0.0856**	**0.8442**	**0.9766**

under segmented in comparison to RIB. The Cellphone image is having textured foreground with shadow in the background. The proposed method attains best values of ME, JI and SA whereas the method [16] attains lowest FNR indicating that the result of the proposed method is under-segmented. The phenomenon can be visualized from Fig. 9 where the result of the proposed method losses the antenna part of the Cellphone. The method LGLD gives the best FPR value for Cellphone image. For 440 image, the proposed method attains lowest ME and SA values, whereas the method [16] and RIB attains best values of FNR, JI and FPR respectively. But, visual representation of segmentation mask in Fig. 10 reveal that the proposed method even if loses some foreground portion removes the background much as compared to existing methods.

To show the effectiveness of the proposed method in comparison with other methods their average performance measure is calculated for all images and are given in Table 3. From Table 3 it is evident that the proposed method has the lowest average ME, FPR, FNR whereas it has highest JI and SA. Hence, the proposed method can be treated as better method as compared to others. The bold values in Table 3 indicate the best values of the performance measures.

6. Conclusion

The proposed method provides a new approach of transition region extraction using fuzzy clustering of local features for image segmentation. The proposed method is robust in the sense that it accurately extracts the accurate transition region irrespective of the background (textured or simple). Experimental results indicate that the proposed method outperform several other methods. The selection of 3-class fuzzy clustering effectively extract transition region thereby improving overall segmentation accuracy. The proposed method works well for both single and multiple objects and the results contain less background regions with little loss of object regions.

References

[1] Mondal S, Bours P. Neurocomputing A study on continuous authentication using a combination of keystroke and mouse biometrics. Neurocomputing 2017;230:1−22. https://doi.org/10.1016/j.neucom.2016.11.031.

[2] Iii WMW, Mondal S, Bours P, Akram T, Naqvi SR, Haider SA, et al. Medical Image Analysis − past, present, and future. Comput Electr Eng 2017;59:1−22. https://doi.org/10.1016/j.neucom.2016.11.031.

[3] Akram T, Naqvi SR, Haider SA, Kamran M. Towards real-time crops surveillance for disease classification: exploiting parallelism in computer vision R. Comput Electr Eng 2017;59:15−26. https://doi.org/10.1016/j.compeleceng.2017.02.020.

[4] Xia Y, Ji Z, Zhang Y. Brain MRI image segmentation based on learning local variational Gaussian mixture models. Neurocomputing 2016;204:189−97. https://doi.org/10.1016/j.neucom.2015.08.125.

[5] Ji Z, Xia Y, Sun Q, Chen Q, Feng D. Adaptive scale fuzzy local Gaussian mixture model for brain MR image segmentation. Neurocomputing 2014;134:60−9. https://doi.org/10.1016/j.neucom.2012.12.067.

[6] Ren Malik. Learning a classification model for segmentation. In: Proceedings ninth IEEE international conference on computer vision, vol. 1. IEEE; 2003. p. 10−7. https://doi.org/10.1109/ICCV.2003.1238308.

[7] Boykov YY, Jolly M-P. Interactive graph cuts for optimal boundary & region segmentation of objects in N-D images. In: Proceedings eighth IEEE international conference on computer vision. ICCV 2001. IEEE Comput. Soc; 2001. p. 105−12. https://doi.org/10.1109/ICCV.2001.937505.

[8] Kim SC, Kang TJ. Texture classification and segmentation using wavelet packet frame and Gaussian mixture model. Pattern Recogn 2007;40:1207−21. https://doi.org/10.1016/j.patcog.2006.09.012.

[9] Zhou Y, Shi W-R, Chen W, Chen Y, Li Y, Tan L-W, et al. Active contours driven by localizing region and edge-based intensity fitting energy with application to segmentation of the left ventricle in cardiac CT images. Neurocomputing 2015;156:199−210. https://doi.org/10.1016/j.neucom.2014.12.061.

[10] Chan TF, Vese LA. Active contours without edges. IEEE Trans Image Process 2001;10:266−77. https://doi.org/10.1109/83.902291.

[11] Chen Y, Zhang J, Mishra A, Yang J. Image segmentation and bias correction via an improved level set method. Neurocomputing 2011;74:3520−30. https://doi.org/10.1016/j.neucom.2011.06.006.

[12] Yan C, Sang N, Zhang T. Local entropy-based transition region extraction and thresholding. Pattern Recogn Lett 2003;24:2935−41. https://doi.org/10.1016/S0167-8655(03)00154-5.

[13] Li Z, Liu C. Gray level difference-based transition region extraction and thresholding. Comput Electr Eng 2009;35:696−704. https://doi.org/10.1016/j.compeleceng.2009.02.001.

[14] Li Z, Zhang D, Xu Y, Liu C. Modified local entropy-based transition region extraction and thresholding. Appl Soft Comput J 2011;11:5630−8. https://doi.org/10.1016/j.asoc.2011.04.001.

[15] Li Z, Liu G, Zhang D, Xu Y. Robust single-object image segmentation based on salient transition region. Pattern Recogn 2016;52:317−31. https://doi.org/10.1016/j.patcog.2015.10.009.

[16] Parida P, Bhoi N. Transition region based single and multiple object segmentation of gray scale images, engineering science and technology. Int J 2016;19:1206−15. https://doi.org/10.1016/j.jestch.2015.12.009.

[17] Parida P, Bhoi N. Wavelet based transition region extraction for image segmentation. Future Comput Inf J 2017;62:119−34. https://doi.org/10.1016/j.fcij.2017.10.005.

[18] Kass M, Witkin A, Terzopoulos D. Snakes: active contour models. Int J Comput Vis 1988;1:321−31. https://doi.org/10.1007/BF00133570.

[19] Yan C, Sang N, Zhang T. Local entropy-based transition region extraction and thresholding. Pattern Recogn Lett 2003;24:2935−41. https://doi.org/10.1016/S0167-8655(03)00154-5.

[20] Parida P, Bhoi N. 2-D Gabor filter based transition region extraction and morphological operation for image segmentation. Comput Electr Eng 2016;0:1−16. https://doi.org/10.1016/j.compeleceng.2016.10.019.

[21] Xu R, WunschII D. Survey of clustering algorithms. IEEE Trans Neural Network 2005;16:645−78. https://doi.org/10.1109/TNN.2005.845141.

[22] Fahad A, Alshatri N, Tari Z, Alamri A, Khalil I, Zomaya AY, et al. A survey of clustering algorithms for big data: taxonomy and empirical analysis. IEEE Trans Emerg Top Comput 2014;2:267−79. https://doi.org/10.1109/TETC.2014.2330519.

[23] Liu T, Yuan Z, Sun J, Wang J, Zheng N, Tang X, et al. Learning to Detect A Salient Object. In: IEEE Transactions on Pattern Analysis and Machine Intelligence, vol. 5555. IEEE; 2010. p. 1−8. http://doi.ieeecomputersociety.org/10.1109/TPAMI.2010.70.

[24] Tarabalka Y, Benediktsson JA, Chanussot J. Spectral-spatial classification of hyperspectral imagery based on partitional clustering techniques. IEEE Trans Geosci Rem Sens 2009;47:2973−87. https://doi.org/10.1109/TGRS.2009.2016214.

[25] Hathaway RJ, Bezdek JC. Fuzzy c-means clustering of incomplete data. IEEE Trans Syst Man Cybern B Cybern 2001;31:735−44. https://doi.org/10.1109/3477.956035.

[26] Yasnoff WA, Mui JK, Bacus JW. Error measures for scene segmentation. Pattern Recogn 1977;9:217−31. https://doi.org/10.1016/0031-3203(77)90006-1.

[27] Sankur B. Survey over image thresholding techniques and quantitative performance evaluation. J Electron Imag 2004;13:146. https://doi.org/10.1117/1.1631315.

[28] Tizhoosh HR, Othman AA. Anatomy-aware measurement of segmentation accuracy. In: Styner MA, Angelini ED, editors. Proc. SPIE 9784, medical imaging 2016. Image Processing; 2016. 97840C. https://doi.org/10.1117/12.2214869.

[29] Rajaby E, Ahadi SM, Aghaeinia H. Robust color image segmentation using fuzzy c-means with weighted hue and intensity. Digit Signal Process 2016;51:170−83. https://doi.org/10.1016/j.dsp.2016.01.010.

[30] Alpert S, Galun M, Brandt A, Basri R. Image segmentation by probabilistic bottom-up aggregation and cue integration. IEEE Trans Pattern Anal Mach Intell 2012;34:315−27. https://doi.org/10.1109/TPAMI.2011.130.